



This is a repository copy of *Tooling materials compatible with carbon fibre composites in a microwave environment*.

White Rose Research Online URL for this paper:
<http://eprints.whiterose.ac.uk/147272/>

Version: Accepted Version

Article:

Nuhiji, B., Swait, T., Bower, M. et al. (3 more authors) (2019) Tooling materials compatible with carbon fibre composites in a microwave environment. *Composites Part B: Engineering*, 163. pp. 769-778. ISSN 1359-8368

<https://doi.org/10.1016/j.compositesb.2019.01.047>

Article available under the terms of the CC-BY-NC-ND licence
(<https://creativecommons.org/licenses/by-nc-nd/4.0/>).

Reuse

This article is distributed under the terms of the Creative Commons Attribution-NonCommercial-NoDerivs (CC BY-NC-ND) licence. This licence only allows you to download this work and share it with others as long as you credit the authors, but you can't change the article in any way or use it commercially. More information and the full terms of the licence here: <https://creativecommons.org/licenses/>

Takedown

If you consider content in White Rose Research Online to be in breach of UK law, please notify us by emailing eprints@whiterose.ac.uk including the URL of the record and the reason for the withdrawal request.



eprints@whiterose.ac.uk
<https://eprints.whiterose.ac.uk/>

Tooling materials compatible with carbon fibre composites in a microwave environment

Betime Nuhiji*^a, Timothy Swait^a, Matthew Bower^a, James E. Green^b, Richard J. Day^c, Richard J. Scaife^a

^a Advanced Manufacturing Research Centre with Boeing, University of Sheffield, Wallis Way, Catcliffe Rotherham, S60 5TZ. E: b.nuhiji@amrc.co.uk

^b Department of Electronic and Electrical Engineering, University of Sheffield, S1 4DE

^c Wrexham Glyndŵr University, Mold Road, Wrexham, Wales, LL11 2AW

Abstract

Although metals are the most commonly used tooling materials to cure composites, they do not provide optimal results in a microwave environment. Following a selection process based on the properties of the materials, an alternative tooling material in carbon fibre reinforced plastic (CFRP) was successfully utilised to cure CFRP panels in laboratory and industrial microwaves. The conductive carbon fibres in the tool facilitated the fast heat transfer across the part. Other tooling materials including a glass fibre cyanate ester prepreg and tooling board were trialled, although the latter exhibited damage during cure. These advantages demonstrate that the CFRP tool is a compatible material that can be used when microwave curing composites.

Keywords: A. Polymer-matrix composites (PMCs), B. Cure behaviour, E. Tooling, Microwave

1. Introduction

Carbon fibre reinforced polymer composites are increasingly being used due to their high strength to low weight properties^[1, 2]. Generally, composites manufacture is conducted using autoclaves, as they provide heat and pressure during cure to yield laminates with low void content and hence the highest strength. Heat transfer in autoclaves is slow as it relies on gas convection and then conduction through the composite as well as tooling and consumables. The long processing times and low efficiency of autoclaves can in turn lead to bottlenecks in production. As the demand for composite structures increases, there is a requirement to develop reliable high-rate manufacturing technologies^[3-5].

Microwave technology can hold significant benefits such as selective, volumetric heating of composite materials, high heating rates (reduction of processing time) and energy efficiency^[6]. To obtain these advantages on an industrial scale without the reduction in composite performance, the manufacturing method must be optimised accordingly. With the focus on tooling materials, a reduction in tooling-part

interaction and increase in the accuracy of composite parts (i.e. coefficient of thermal expansion (CTE)) can be achieved by optimising the tooling materials and design for manufacture^[7].

Polymers and composites have been manufactured in microwaves on a laboratory scale, where tools such as quartz/glass^[8, 9], polytetrafluoroethylene (PTFE)^[10-16] and ceramics such as Macor[®]^[17, 18] have been used. PTFE has a high service temperature (300 °C) and low dielectric loss factor^[19] although it is geometrically unstable. Macor[®] based ceramics are machinable, exhibit good dielectric properties and dimensional stability, but are expensive for larger scale applications as are glass/quartz materials. These materials prove desirable in a microwave environment, although they do not meet the industrial requirements, particularly robustness and practicality.

Manufacturing composites in an industrial microwave have seen the likes of metallic tooling being utilised^[6, 20, 21] alongside glass^[22-24] and composite^[7]. Although metal tools are commonly used to cure composites in autoclaves, they do not provide optimal results when microwave curing a composite, as they reflect electromagnetic (EM) radiation and lead to arcing^[25], have very high thermal conductivity and act as a heat sink drawing energy from the material. Other bespoke tooling combinations have also been explored. GKN Aerospace have developed tools consisting of Invar as the bulk with the addition of a carbon fibre laminate surface^[26]. TWI have researched a microwave tooling material, MU-TOOL^[27], where the bulk material is microwave transparent, with an absorbing layer on the tool surface.

Although research is being conducted in the area of tooling materials for microwave curing, there is still a lack of experimental data restricting development of robust and optimised processes for better repeatability^[25]. A selection of tooling materials commonly used in engineering practise for composite manufacture are investigated in this paper, with a focus on curing CFRP laminates using laboratory and industrial scale microwave systems. The dielectric and thermal diffusivity properties of the tools provide data on their heating capabilities when exposed to EM radiation, whereas the microwave trials explored the heat distribution of the laminates and tools during cure. Tool damage was assessed as was the laminates state of cure.

2. Materials and methods

2.1 Materials and manufacturing

Two microwaves were used in this study: a test bed and an industrial Vötsch HEPHAISTOS VHM

180/200 system. Both microwaves operate at a frequency of 2.45 GHz and can control (from highest reading) and monitor temperature using fibre optic thermosensors (FOT's). The test bed is based on a Panasonic NN-CF778 system and uses a bespoke control designed to cure composite materials [28]. The EM field is generated by a single magnetron (1 kW). The Vötsch system has 24 magnetrons positioned in a hexagonal configuration with a total maximum power of 21 kW and has two infrared (IR) cameras to view the heat distribution of a composite within the chamber. The design was established to improve field homogeneity [6], where fans are located in the top of the cavity to facilitate forced convection cooling. A schematic illustration of the Vötsch microwave system is shown in Figure 1.

Test bed trials were conducted on CFRP laminates consisting of 190 mm x 190 mm Cycom 5320-1 T650 3K plain weave prepreg. The geometry for industrial trials comprised of a flat surface in the centre and two hemispheres used to identify how the complexity in shape affects the EM field. Panels consisted of 8 plies [0/90]_s that were shielded with aluminium tape to avoid potential arcing and bagged using release film, sealant tape, glass fibre breather and an elastomeric vacuum bag. All panels were cured using the manufactures schedule (121 °C for 180 minutes; 177 °C for 120 minutes) with the addition of a 3 °C/minute ramp rate.

Tooling materials include carbon fibre/epoxy tooling prepreg, glass fibre/epoxy prepreg, glass fibre/cyanate ester prepreg, high temperature tooling board (Trelleborg TC460) and Ultem™ thermoplastic. The three composite based tools were manufactured with stacks of pre-impregnated woven material (anisotropic due to the various fibre directions) and processed using conventional methods (autoclaves and ovens). These materials are used widely within the composite industry as tooling for CFRP components. The TC460 tooling board is a commercially available material used extensively in the processing of composite materials at elevated temperatures. It consists of a low density syntactic epoxy material. Ultem™ is a commercially available thermoplastic polyetherimide based polymer system that is suitable for high temperature applications and is typically microwave transparent. The Ultem™ panels in this study were processed using 3D printing and were post cured to improve the stability of the polymer at higher operating temperatures. All of these tools were cleaned, sealed and released in a similar manner to when curing composites and therefore did not present any issues when releasing the tools from their respective CFRP parts. Composites were processed according to

manufacturer's guidelines, whereas the tooling board and Ultem™ materials were used as they were supplied. Their size was dependant on the scale of the trials: tools used in the test bed were 300 mm x 300 mm, whereas the design dimensions for the larger scale were 1500 mm x 600 mm x 95 mm. The features of the large tool include a flat surface in the centre and two hemispheres (to identify how the complexity in shape affects the EM field). The tool also had concave and convex fillets on the steps of two different radii and a planar symmetry. Note that the tools were only cycled once during the industrial trials, although on multiple occasions for the test bed trials.

2.2 Characterisation

Dielectric and thermal diffusivity properties were measured and used to select candidate tooling materials. Differential scanning calorimetry (DSC) was used to evaluate the composites degree of cure, while micrographs were taken to view damage to the tools.

2.2.1 Dielectric properties

The form of the tooling materials dictated how their dielectric properties were measured. Laminar materials of thicknesses < 2 mm required the use of a mode cavity method (Split-Post Dielectric Resonator (SPDR)), whereas non-laminar materials were measured using a resonance cavity perturbation method, as they could be contained within a sample tube^[29].

The SPDR measurements were made using a commercial jig from Quickwave, operating in TE₀₁₁ mode at 2.493 GHz, and an Anritsu Scorpion vector network analyser. The thickness of the samples were measured in at least three regions and averaged. The resonant frequency and Q were measured with and without the sample, and dielectric properties were calculated via Quickwave's proprietary software. Cavity perturbation measurements were made using a microwave calorimeter developed by Nesbitt et al.^[30]. This is based on a single mode resonant cavity operating in the TE₁₁₁ mode with resonant frequency of approximately 2.45 GHz, depending upon the nature and quantity of the sample present. The cavity had a radius of 58 mm and height of 77 mm. A sample tube holder (Ø10 mm OD, 8 mm ID) was located at the centre of the cavity so that the sample was in the area of maximum electric field. An amplifier (Microwave Amplifiers Ltd) was placed in the system, with a network analyser (HP 8720ET). The resonant frequency and Q are measured for the empty cavity with and without the sample, where the complex dielectric properties were then calculated from Equations 1 and 2^[30].

$$\varepsilon' - 1 = A \frac{(f_c - f_s) V_c}{f_c V_s} \quad \text{Eq. 1}$$

$$\varepsilon'' = B \left(\frac{1}{Q_s} - \frac{1}{Q_c} \right) \frac{V_c}{V_s} \quad \text{Eq. 2}$$

ε' and ε'' represent the dielectric permittivity and loss, respectively, f_c and f_s are the values of the cavity and sample frequencies (Hz), Q_c and Q_s are the Q factors for the cavity and samples and V_c and V_s are the volumes (m^3) of the cavity and samples, respectively. A and B are variables that are dependent upon the geometry and dielectric properties of the sample, the geometry of the cavity and the temperature within the cavity [31]. Calculation of these variables is possible in a limited number of cases. In most cases the values of A and B are found by calibration, all measurements are conducted at room temperature (20 °C) to limit the variation of A and B. In this case the cavity was calibrated against samples of PEEK which has similar dielectric properties to the materials measured in this study.

2.2.2 Thermal diffusivity

The thermal diffusivity of a material determines how it responds to a change in temperature and is the thermal conductivity divided by the volumetric specific heat capacity (Eq.3).

$$\alpha = \frac{k}{\rho C_p} \quad \text{Eq. 3}$$

α is the thermal diffusivity, k is conductivity ($\text{W}/(\text{m}\cdot\text{K})$), ρ is the density (kg/m^3) and C_p is the specific heat capacity ($\text{J}/(\text{kg}\cdot\text{K})$). Volumetric specific heat can be stated as density and specific heat of a material (ρC_p).

The diffusivity of all tooling materials was measured using a TPS2500S HotDisk. The direction that the heat is transferred for anisotropic materials was expressed in terms of the axial and radial orientations, where the axial direction is through the thickness of a sample, and the radial is across its plane. Results were interpreted with the Thermal Constants Analyser 7.2.6 software.

2.2.3 Differential scanning calorimetry (DSC)

A Perkin Elmer DSC 4000 was used to measure the heat capacity evolved in an as-received sample of Cycom 5320-1 prepreg and any residual cure within CFRP parts cured using microwaves. Composite sections were oven dried overnight to remove any moisture and tested three times for repeatability. To measure the heat capacity as well as the residual cure of the as-received prepreg and the CFRP parts, respectively, samples were heated to 300 °C at 10 °C/minute and cooled to room temperature. Once conducted, the CFRP parts were analysed for their degree of cure (DOC) using Equation 4.

$$DoC = \frac{\delta H(r) - \delta H(T)}{\delta H(T)} \times 100\% \quad \text{Eq. 4}$$

$\delta H(T)$ is the total heat of reaction (J/g) and $\delta H(r)$ is the residual heat of reaction (J/g).

2.2.4 Optical microscopy

A Zeiss Stemi 2000-C optical microscope with AxioCam ERc-5c digital camera was used to take micrographs of the damage exhibited in the tooling materials once they had undergone microwave processing. Images were analysed via AxioVision software.

3. Results and Discussion

3.1 Material selection via dielectric and thermal diffusivity properties

The dielectric and thermal diffusivity properties of eight tooling materials are shown in Table 1. These consist of materials that have traditionally been used for laboratory scale trials (glass, ceramic and PTFE) as well as industrial based tools for conventional curing (CFRP and glass fibre reinforced epoxy (GFRE) composites and tooling board). A glass fibre reinforced cyanate ester composite (GFRCE) and a thermoplastic, Ultem™, were also selected. Note that the dielectric measurements of materials such as borosilicate glass and Macor® were sourced^[32, 33]. Specific heat, density and conductivity measurements were taken from literature and used with Eq.3 to calculate their thermal diffusivity properties. The CFRP prepreg is a conducting material that cannot be measured for dielectric properties.

The combination of dielectric and thermal diffusivity properties provide the following knowledge; dielectric permittivity is the measure of how much energy is stored in a material, while dielectric loss specifies the amount of heat a material can generate and the thermal diffusivity denotes how fast this heat can transfer through the material. For dielectric loss, Metaxis and Meredith have stated that as a general rule, a material can be heated using microwaves when this property is between 0.01 – 5^[34].

From the data in Table 1, borosilicate glass, Macor® and PTFE attain desirable properties as microwave tools in that they are transparent to irradiation ($\epsilon'' < 0.01$), where only the composite material would be heated. Although this notion is plausible, a composite panel can lose heat to the external environment making it difficult to reach the cure temperatures required. Alternatively, tooling materials that absorb irradiation can transfer some heat to a composite during cure. From the dielectric loss properties in Table 1, the tools that can generate heat are highlighted: GFRCE, GFRE and CFRP composites

as well as TC460 tooling board and Ultem™. These tooling materials also exhibit similar ϵ' values to the transparent tools. In regards to thermal diffusivity properties, the CFRP composite conducts heat more effectively than the resin itself.

3.2 Test bed trials

Figure 2 shows temperature-time-power graphs of CFRP panels being cured via a) CFRP b) Ultem™ c) GFRCE and d) TC460 tools. FOTs were placed in the same location on the laminates and tools for each trial. FOT-A is in between the laminate and tool, FOT-B is positioned below the tool and FOT-C is measuring the temperature of the laminate surface. Although the GFRE composite tool was trialled in a microwave, it was not suitable due to the extent of the damage that it experienced. The damage was initiated from a combination of factors including suspected stray carbon fibres, EM field concentration and void content. Stray carbon fibres in a glass composite can lead to arcing which instigates damage, as discussed by Teufl and Zaremba^[22]. From Figure 2, three out of the four tools all underwent the full cure namely CFRP, Ultem™ and GFRCE. During each cure, the power level remained at ~50 % and both the laminate and tools followed the set temperatures to within 2 – 7 °C for the initial stage.

3.2.1 CFRP tool

The CFRP tooling material combined with the CFRP panel performed well with a maximum temperature gradient of 10 °C across all of the FOT's (Figure 2a). Although there was one arc observed at the beginning of the cycle, partial vacuum (~50 mbar) was still maintained throughout the cure and there were no signs of burning to the tool or panel.

3.2.2 Ultem™ tool

The heating behaviour of the Ultem™ (Figure 2b) can be explained by the transparency property that the tool exhibits, as the ϵ'' is low at 0.011. At the beginning of the cure cycle, the Ultem™ tool surface remains the coldest with a thermal lag of ~10 °C between tool and laminate surfaces (FOT-B and FOT-C), which is then reversed throughout the initial temperature sweep. This phenomenon is observed as the Ultem™ has a low relative dielectric loss factor, indicating the tool does not absorb microwave energy in the initial stages of processing. However, later in the cure as heat is dissipated into the material from the CFRP composite (via conduction), the Ultem™ heats and is unable to disperse this thermal energy (as seen by the low thermal diffusivity) leading to the thermal overshoot. Even though the microwave source is

located at the bottom (the system contains a bottom up heating mechanism where the antenna and mode stirrer are located under the base plate of the cavity) the tool did not appear to experience the same heat as the CFRP panel. At 90 °C (~30 minutes), however, the Ultem™ material experienced a rapid rise in temperature. When the microwave control system stopped providing energy, the recorded tool temperature continued to increase. This effect can be noticed during the first and second ramp cycles. It is also worth noting that the tooling surface remains the hottest throughout the cycle, even though it initially was cooler. Given the unexpected behaviour of the Ultem™, the tool was evaluated using DSC to identify whether there was a reaction occurring within this material. It was compared to an Ultem™ tool that had not been exposed to microwave irradiation. Both the tools did not exhibit any reactions between room temperature and 200 °C and therefore the rapid rise in temperature cannot be attributed to residual reaction heat within the material. This uncontrolled temperature runaway does not make the tool suitable for industrial trials.

3.2.3 GFRCE tool

From Figure 2c, all of the FOT's measured similar temperatures during the initial heating stage. This differed during the dwell, where the surface of the laminate (FOT-C) remained the coldest of the tools trialled, although the tool itself was following the set temperature. The temperature gradient between both surfaces measured to within a maximum of 7 °C where the greatest amount of heat was located at the tool surface. This result could be explained by the microwave configuration, with the heating mechanism at the cavity surface. The post cure shows a similar pattern to that of the initial cure where the higher temperatures are exhibited on the tooling surfaces rather than the laminate, which again is a contributing factor from the location of microwave source. The temperature gradient between the surfaces was within a maximum of 7 °C throughout the cure cycle.

3.2.4 TC460 tool

From Figure 2d, the TC460 tool (FOT-B) heated at a quicker rate than the CFRP panel (FOT-C) resulting in a temperature gradient of ~10 °C between the tool and laminate surfaces. Once the temperature of the TC460 tool overshoot the dwell set point (120 °C), the magnetron switched off although the tool continued to heat. Again this effect could be due to the heat transfer from areas of the tool that were not being monitored. The trial was then ceased. Relating these observations to the dielectric and diffusivity

properties, the ϵ'' is comparable to the GFRCE tool, although the diffusivity is 50 % lower meaning that the heat does not transfer well along the material.

3.2.5 Damage experienced in the tools

Of the tools trialled in the microwave test bed, GFRCE and TC460 exhibited the greatest damage (Figure 3). For GFRCE, the damage is located where the CFRP panel edges experienced localised heating and in turn, arcing that occurred at the start of the cycle. This damage can be seen as a discoloured region in the optical micrograph (Figure 3a_{ii}). When magnified further, it is evident from the cross-section that voids are present within the composite although there does not appear to be any delamination.

Alternatively, the damage exhibited in the TC460 tool is far greater in the form of a significant crack, including discolouration. It appears that the material began to burn from its centre rather than its surfaces. Once a hotspot was initiated, the energy may have been drawn to the damaged region as it charred and the electrical conductivity increased, which would then accelerate the decomposition of the tool. Optical micrographs of the fractured material surfaces (Figure 3b_{ii}&iii) capture the discoloured regions appearing from within the crack and display the burnt surface that was fractured.

Table 2 summarises the performance of the five tooling materials that were trialled in the microwave test bed. From this data, the only tooling material in this trial that could withstand a microwave cure cycle without experiencing any damage was the CFRP composite. Combined with a CFRP panel, the materials provided a greater conducting/absorbing load for the microwave, as well as the benefit of attaining similar CTE properties. Given the success of this tool during the three trials, this material was tested on an industrial scale (Section 3.3.1). The GFRCE composite and Ultem™ tools could also withstand the cure cycle. The trials for GFRE and TC460 tools were ceased: of these tools, GFRCE and TC460 tools exhibited damage that can be attributed to the test beds heating mechanism leading to localised heating and hot spots in selected regions. Given that the heating mechanism of the Vötsch system differs from the test bed, it was of interest to trial the TC460 and GFRCE materials on an industrial scale. In regards to the Ultem™, the materials unusual and uncontrollable behaviour at approximately 90 °C and 160 °C (Figure 2) as well as its hydroscopic nature made it unsuitable for industrial trials.

3.3 Industrial trials

Three large scale tools were manufactured: 1) CFRP/epoxy prepreg, 2) TC460 board as well as 3)

GFRP/cyanate ester (GFRCE) according to the geometry outlined in Section 2.1.

3.3.1 CFRP tool

Shown in Figure 4 are the results from the microwave trial conducted using a CFRP tool and panel. These include the location of metallic K-type thermocouples (referred to throughout the study as thermocouples) and FOT's (a), a captured IR image during cure (b) and the temperature-time-power graph of the cycle (c).

Results of the first stage cure cycle are shown in Figure 4c, where temperatures are monitored using a total of eight thermosensors (five thermocouples and three FOT's). The thermocouples were used to measure the temperature between the tool and the laminate, whereas the FOT's measure the temperature on the laminates surface. From the data shown in Figure 4c, the highest temperature recorded was at the thermocouple, TC3 (located on the flat surface). This thermocouple (alongside TC2) continued to follow the set point during the 3 hour dwell. Of the thermocouples, the temperature gradient was ~ 10 °C across the laminate. For the FOT's, the highest temperature monitored was located at the concave hemisphere via FOT-A (~ 117 °C). When comparing FOT-A to the other FOT's, the difference in temperature reading was 13 °C, where the FOT measuring the lowest temperature was located at the convex hemisphere (FOT-C).

To visualise the results, an infrared (IR) image was taken during cure (Figure 4b). The IR cameras capture the heat evolving from the tool and laminate, where regions experiencing greater temperatures are displayed as a brighter yellow/orange colour. The chequerboard pattern in the IR image is an artefact of the grid in the ceiling of the microwave cavity that the camera is positioned behind. Thermocouples provide readings that need to take into consideration four factors: 1) the probes act as antennae, 2) the aluminium shielding can potentially cause arcing, 3) they are good thermal conductors affecting the temperature distribution and 4) the probes can form a ground affecting the local electric field strength. FOT's provide clearer information, given their dielectric transparency characteristics within a microwave environment. As can be seen in the IR image (Figure 4b), although TC2 and TC3 measured the highest temperature (and were, therefore, used for control (Figure 4c)), the heat was being transferred from the shielding of the thermocouples. This can also be seen with the other thermocouples, TC4, TC5 and TC6. Apart from the thermocouples, there is a noticeable hot region located at the concave hemisphere in

comparison to the flat and convex surfaces (circled). This correlates well with the FOT temperature readings (Figure 4c).

When collating information, FOT-B and TC6 exhibit similar temperatures and they are located in the same region (flat surface), although TC6 is higher given that the heat remains between the tool and laminate since the former has lower thermal diffusivity. FOT-B remains slightly cooler since it is on the laminates surface and the exhaust fan of the microwave was operating which will have created airflow across the surface. The full cure cycle was not achieved as it was ceased due to a smoulder located at a thermocouples. Given this, only FOTs were used to post cure the laminate. Figure 4c also displays the temperature-time-power graph of the results from the post cure. The highest temperature reading was registered as FOT-A (centre of the laminate), followed by FOT-B and FOT-C, respectively. The temperature gradient across the laminate is 13 °C, which is consistent with the gradient in the first stage cure, although the power consumption increases from the first stage cure (30 %) to an average of 50 % for the post cure. The panel was post cured successfully (80 mbar vacuum pressure) without experiencing any damage to the tool. Apart from the initial issues caused by the thermocouples, the CFRP tool performed well within the test bed as well as the industrial Vötsch system.

3.3.2 GFRCE tool

GFRCE material was laminated onto the CFRP tool and cured in an autoclave, followed by a free standing post cure (2 hours at 250 °C). Unlike the CFRP tool, only FOT's were used to control and measure temperature for the GFRCE. All three FOT's were located in the centre of the generic designed laminate/tool, with FOT-A on the laminate surface, FOT-B positioned in between the laminate and tool and FOT-C on the tool surface (Figure 5a).

The cure results for this trial are shown in Figure 5c as part of a temperature-time-power graph. From this information, FOT-B measured the highest temperature throughout the cycle followed by FOT-A (~10 °C gradient) and FOT-C (~20 °C gradient). This can be explained by the locations of the FOT's in relation to the materials and set up in the Vötsch system. Thermosensor FOT-B is measuring the highest temperature. An interesting result is that of FOT-C (tool surface), is the coldest of all locations. When conducting the test bed trials, the temperature of the FOT on the surface of the CFRP was 7 °C lower than between the tool and laminate (Figure 2c). This difference in heating mechanism from the test bed and

the Vötsch can assist in explaining these results. The test bed introduces EM energy from the bottom plate^[28] and when the GFRCE tool/CFRP laminate was trialled, heat was being transferred from the tool to the laminate. Alternatively, the EM radiation introduced into the Vötsch system is via a hexagonal configuration and not just from the one region (with one source). This configuration is much more representative to industrial production.

An IR image of the heat distribution across the GFRCE tool/CFRP laminate is presented in Figure 5b. From this image, there are two regions of localised heat throughout the laminate: the concave hemisphere as well as a position close to the convex hemisphere (refer to Figure 5a). Although the temperature at these locations was not directly measured during cure, it is worth noting that there were no heating induced issues with the thermocouples, since only FOTs were used. Hence, these hot zones represent degrees of inhomogeneity in the heating. Once the CFRP laminate was cured, the panel and tool were de-bagged and inspected. The vacuum pressure was held constant at 80 mbar throughout the cure and there were no issues experienced during the cycle.

Figure 5d displays (a) the final CFRP product and the GFRCE tool alongside images of the damage that was noticed to the CFRP panel (i) and the tool (ii). When relating these images to those captured via the IR cameras (Figure 5b), it is evident that the damage to the tool was due to excessive heat being localised at the positions outlined. The CFRP panel also shows damage in the concave location. These findings are similar to the results demonstrated in the test bed (Section 3.2), where the tool showed signs of discolouration. When analysing the tool using microscopy, there were voids present (Figure 3a).

3.3.3 TC460 tool

TC460 tooling board was machined using 5-Axis Ares CMS CNC machine to achieve the same profile as used in the other industrial trials. The tool was constructed using two 50 mm blocks adhered together with high temperature epoxy resin (EP661). Temperatures were measured in the same position as the trial with the GFRCE tool: the flat section of the laminate/tool with FOT-A on the laminate surface, FOT-B positioned in between the laminate and tool and FOT-C on the tool surface.

Figure 6b shows an IR image of the heat distribution that the materials experienced during cure. From the image, the heat is distributed well across the whole laminate, although the bottom half and concave hemispherical region (top) appear to exhibit greater localised heat shown by the bright yellow colour. The

heat at the concave region is similar to the laminates cured on the CFRP and GFRCE tools. Given that all of the industrial geometries are experiencing this localised heating suggests that there is a build-up of EM field in the concave region and that the field is stronger at this point.

A temperature-time-power graph of the cure cycle is shown in Figure 6c. FOT-C (tool surface) acted as the control thermosensor as it remained at the highest temperature during cure, and was continuously measuring over the set point of 121 °C at the dwell stage. FOT-A and FOT-B show a similar temperature profile to one another, although FOT-A was located on top of the laminate where the exhaust air circulates through the chamber and remains cooler. In terms of temperature gradients, there was a 20 °C difference from the tool surface to that of the laminate surface and although the temperature of the tool increases slightly midway through the dwell (by 1 °C), the laminate heat decreases.

Of interest is the power profile in Figure 6c, as there are two surges of energy during the initial ramp (75 % and 90 %, respectively) although during the dwell, the system does not require further power to heat the tool. On the second surge, the temperature of the tool increases and overshoots past its set point, whilst the laminate remains at a constant heat going forward. Given that the tool appears to still remain above the temperature set point and not cool, suggests that the heat is diffusing from areas of the tool that were not being measured. Note that the microwave was switched off midway through the cycle, due to a slight odour within the first hour of dwell.

When comparing the temperature-time-power graphs between the test bed trial in Figure 2 and the Vötsch system (Figure 6), the tool surface experienced the greatest heat although the temperature of the interface between tool and laminate remained higher than the laminate surface temperature. The heat experienced by the tool surface is an appealing result, as the heating mechanism for the Vötsch system is not bottom fed unlike the test bed. Alternatively, the reason for the laminate remaining cooler is due to the fan-forced air in the cavity. In regards to the tool damage, it is evident from Figure 6d that the tool is cracked on the flat surface (highlighted in a circle). The crack propagates around the concave hemisphere region and through the centre of the tool (i, ii). The cracks are accompanied by discolouration where the adhesive was located to combine the tooling blocks. These findings are similar to the trials conducted in the test bed, where cracks and heat influenced damage were evident in the tooling board (Figure 3b). To summarise these results, it is believed that there are several reasons for the damage including the use of

a faster heating rate (3 °C/minute and not the recommended 0.15 °C/minute), the inclusion of titania particles and epoxy adhesive adding to the absorption characteristics, as well as any runaway reaction occurring once a hot spot has been initiated. It is for these reasons that the TC460 tool cannot be considered as a feasible high temperature material for microwaving composites.

3.3.4 Differential Scanning Calorimetry

The CFRP panels cured in the Vötsch were analysed using DSC to establish their degree of cure (DOC). The enthalpy of reaction of as-received Cycom 5320-1 prepreg was 181 J/g. The panels cured using each tool were tested at a number of locations across the part to evaluate their DOC (Figure 7a for regions 1-6). These locations refer to regions where FOT's and/or thermocouples were placed so that representative data could be attained. The corresponding table summarises the DOC values for each CFRP panel microwave cured on a CFRP and GFRCE tool alongside the DOC from the manufacturers. All of the tests were conducted to provide an indication of the cure homogeneity. Note that a cured composite panel was not manufactured using the TC460 tool and therefore did not undergo DSC trials. A few observations can be deduced from Figure 7 such as 1) the minimum and maximum DOC values for both panels were 76 % and 99 %, respectively, 2) variations throughout each panel are 76 % - 99 % for GFRCE and 84 % - 95 % for CFRP and 3) a similar pattern emerges for both panels, where the highest DOC was located in the centre of the geometry (flat section) ranging from 87 % - 99 %, and the lowest DOC value was situated at the convex hemisphere (76 % - 84 %). Of interest is that the DOC remains higher at the concave hemisphere than that of the convex. These results can be correlated to the respective IR images taken of each panel in Figure 4b and Figure 5b, where hot spots in these images are highlighted at the concave hemisphere.

An interesting observation occurred at the hemispheres during a cure cycle. Regardless of the tooling material used, there was greater heat generated in/around the concave hemisphere in comparison to that of the convex. This result is supported by the DOC values calculated. It is hypothesised that the concave region induces a lens effect throughout the cure cycle that focuses incident microwaves into its centre. The lens effect can also be used to describe the blistering and discolouration seen in Figure 5d for the GFRCE tool and panel, respectively.

When referring to the microwave cured panels, the average DOC show similar results with a difference of only 2 %. Although this difference is minimal, the uniformity across each panel needs to be taken into consideration for the quality of the overall part, therefore suggesting that the CFRP tool is the most suitable for microwave cure (only 11 % DOC variation compared to 23 %). When comparing the average DOC values of the microwave cured parts to that of the manufacturer's (95 %), the microwaved panels exhibited variation in results. The authors are conducting further work to reduce this variability, where a variety of methods have been identified in the literature that could be used to analyse the uncertainties within the process ^[35, 36].

4. Conclusion

The work focused on selecting commercially available tooling materials suitable for use in an industrial microwave. Of the materials initially scoped, only CFRP and GFRCE tools were able to successfully cure CFRP panels in both a test bed and Vötsch microwave. A suitable tooling material that is capable of being used within a microwave environment must have a variety of qualities such as being robust and practicable, easy to machine/mould, and readily available. The performance of the tools can be qualified in terms of temperature gradients, degree of cure as well as any damage exhibited. From this, the average DOC values of CFRP and GFRCE tools are similar. The GFRCE tool, however, had a DOC difference of 23 % in comparison to CFRP @ 11 % across the part, showing that the CFRP tool has less variation in cure. This variation within GFRCE could be due to the lower heat transfer axially (through thickness) and radially (along fibres) in the tool. In terms of the processability of the tools on a larger scale, the CFRP and GFRCE are comparable in terms of cost (~£50/m² for CFRP and ~£75/m² for GFRCE). However, the GFRCE is significantly more challenging to manufacture with a higher processing temperature (250 °) that requires advanced auxiliary processing materials and greater control of the production process to avoid significant moisture absorption and contamination. The CFRP tool did not exhibit damage, the CTE matches that of the panel and the material is readily available. These advantages demonstrate that the CFRP tool is a compatible material that can be used for multiple cycles when microwave curing composites. The authors are currently exploring multiphysics computational methods for simulating the microwave cavity to assess the underlying physics within the curing process and to validate experimental results ^[36, 37].

5. Acknowledgements

This work was supported by the AMRC industrial members, where the authors sincerely appreciate the continuous support provided. The authors would also like to thank the Cytec Solvay group for supplying carbon fibre prepreg and gratefully acknowledge the assistance from Tim Mann on the thermal diffusivity tests. Day was supported by an EPSRC High Value Manufacturing Catapult fellowship (EP/L017121/1).

6. References

- [1] Cai H, Aref AJ. On the design and optimization of hybrid carbon fiber reinforced polymer-steel cable system for cable-stayed bridges. *Composites: Part B*. 2015;68:146–52.
- [2] Kwan-WooKim, Dong-KyuKim, young-SuhkKim, Kay-HyeokAn, Soo-JinPark, YopRhee K, et al. Cure behaviors and mechanical properties of carbon fiber-reinforced nylon6/epoxy blended matrix composites. *Composites Part B: Engineering*. 2017;112:15-21.
- [3] Severijns C, Freitas STd, Poulis JA. Susceptor-assisted induction curing behaviour of a two component epoxy paste adhesive for aerospace applications. *International Journal of Adhesion and Adhesives*. 2017;75:155–64.
- [4] Wu Q, Ma L, Wu L, Xiong J. A novel strengthening method for carbon fiber composite lattice truss. *Composite Structures*. 2016;153:585–92.
- [5] Nuhiji B, Attard D, Deveth A, Fox B. The influence of processing techniques on the matrix distribution and filtration of clay in a fibre reinforced nanocomposite. *Composites Part B: Engineering*. 2016;84(1-8).
- [6] Feher LE, Thumm MK. Microwave innovation for industrial composite fabrication - the HEPHAISTOS technology. *IEEE Transactions on plasma science*. 2004;32(1):73 -9.
- [7] Li Y, Li N, Gao J. Tooling Design and Microwave Curing Technologies for the Manufacturing of Fiber-reinforced Polymer Composites in Aerospace Applications *The Int Journal of Adv Manufacturing Tech*. 2014;70(1-4):591-606.
- [8] Paulauskas FL. Variable frequency microwave curing, processing of thermoset prepreg laminates: Oak Ridge National Laboratory; 1997.
- [9] Thostenson ET, Chou TW. Microwave and Conventional Curing of Thick-Section Thermoset Composite Laminates: Experiment and Simulation. *Polymer Composites*. 2001;22(2):197 - 212.
- [10] Yusoff R, Aroua MK, Nesbitt A, Day RJ. Curing of polymeric composites using microwave resin transfer moulding (RTM). *Journal of Engineering Science and Technology*. 2007;2(2):151-63.
- [11] Jullien H, Valot H. Behaviour of film-forming polymers in a microwave electric field. *Polymer*. 1983;24:810 - 4.
- [12] Bai SL, Djafari V. Interfacial properties of microwave cured composites. *Composites*. 1995;26(9):645-51.
- [13] Fang X, Scola DA. Investigation of Microwave Energy to Cure Carbon Fiber Reinforced Phenylethynyl-Terminated Polyimide Composites, PETI-5/IM7. *Journal of Polymer Science: Part A: Polymer Chemistry*. 1999;37:4616–28.
- [14] Lee W, Springer GS. Microwave curing of composites. *Journal of Composite Materials*. 1984;18:387 - 409.
- [15] Nightingale C, Day RJ. Flexural and interlaminar shear strength properties of carbon fibre/epoxy composites cured thermally and with microwave radiation. *Composites Part A: applied science and manufacturing*. 2002;33(7):1021-30.

- [16] Mooteri PS, Sridhara BK. Studies on Mechanical Behavior of Microwave and Thermally Cured Glass Fiber Reinforced Polymer Composites. *Journal of reinforced plastics and composites*. 2006;25(5):501 -12.
- [17] Papargyris DA, Day RJ, Nesbitt A, Bakavos D. Comparison of the mechanical and physical properties of a carbon fibre epoxy composite manufactured by resin transfer moulding using conventional and microwave heating. *Composites Science and Technology*. 2008;68(7-8):1854-61.
- [18] Li N, Li Y, Hang X, Gao J. Analysis and optimization of temperature distribution in carbon fibre reinforced composite materials during microwave curing process. *Journal of Materials Processing Technology*. 2014;214:544-50.
- [19] Ahmad Z. *Polymeric Dielectric Materials*. Dielectric Material: INTECH; 2012.
- [20] Kwak M, Robinson P, Bismarck A, Wise R. Microwave curing of carbon–epoxy composites: Penetration depth and material characterisation. *Composites Part A: applied science and manufacturing*. 2015;75:18-27.
- [21] Li N, Li Y, Wu X, Hao X. Tool-part interaction in composites microwave curing: Experimental investigation and analysis. *Journal of Composite Materials*. 2017;51(26).
- [22] Teufl D, Zaremba S. 2.45 GHz Microwave Processing and Its Influence on Glass Fiber Reinforced Plastics. *Materials*. 2018;11(5):838.
- [23] Hang X, Li Y, Hao X, Li N, YouyiWen. Effects of temperature profiles of microwave curing processes on mechanical properties of carbon fibre–reinforced composites. *J Engineering Manufacture*. 2017;231(8):1332–40.
- [24] Li N, Li Y, Jelonnek J, Link G, Gao J. A new process control method for microwave curing of carbon fibre reinforced composites in aerospace application. *Composites Part B*. 2017;122:61-70.
- [25] Mishra RR, Sharma AK. Microwave–material interaction phenomena: Heating mechanisms, challenges and opportunities in material processing. *Composites: Part A*. 2016;81:78–97.
- [26] Sloan J. Microwave: An alternative to the autoclave? Aerospace composites manufacturer GKN evaluates microwave oven practicality and cost-effectiveness.: *CompositesWorld*; 2011.
- [27] TWI, Microcab, Loiretech, Neosid, Nanotechnology S, Gmbh JC, et al. *Mu-Tool: Novel tooling for composites curing under microwave heating*. France: European Commision (FP7-SME 2012).
- [28] Green JE, Nuhiji B, Zivtins K, Bower MP, Grainger RV, Day RJ, et al. Internal Model Control of a Domestic Microwave for Carbon Composite Curing. *IEEE Transactions on Microwave Theory and Techniques*. 2017.
- [29] Clarke B. *A guide to characterisation of dielectric materials at RF and microwave frequencies*. 2003.
- [30] Nesbitt A, Navabpour P, Degamber B, Nightingale C, Mann T, Fernando G, et al. Development of a microwave calorimeter for simultaneous thermal analysis, infrared spectroscopy and dielectric measurements. *Measurement Science and Technology*. 2004;15:2313-24.
- [31] Cuenca J, Slocombe D, Porch A. Temperature Correction for Cylindrical Cavity Perturbation Measurements. *IEEE Transactions on Microwave Theory and Techniques*. 2017;65(6):2153-61.
- [32] Cuming E. *Dielectric material chart - ECCOSTOCK® Low Loss Dielectrics & Other Common Materials*
- [33] Soldatov S, Kayser T, Link G, Seitz T, Layer S, Jelonnek J. Microwave cavity perturbation technique for high temperature dielectric measurements In: *Proceedings of Microwave Symposium Digest (IMS), 2013 IEEE MTT-S International*. Seattle, Washington, Conference, Conference 2013. p. 1-4.
- [34] Metaxas AC, Meredith RJ. *Industrial Microwave Heating 1983*; IET Power and Energy Ed.

[35] Hamdia K, Silani M, Zhaung X, He P, Rabczuk T. Stochastic analysis of the fracture toughness of polymeric nanoparticle composites using polynomia chaos expansions. *International Journal of Fracture*. 2017;206:215-27.

[36] Msek M, Cuong NH, Zi G, Areias P, Zhuang X, Rabczuk T. Fracture properties prediction of clay/epoxy nanocomposites with interphase zones using a phase field model. *Engineering Fracture Mechanics*. 2018;188:287-99.

[37] Hamdia K, Zhuang X, He P, Rabczuk T. Fracture toughness of polymeric particle nanocomposites: Evaluation of models performance using Bayesian method. *Composites Science and Technology*. 2016;126:122-129

7. Figures

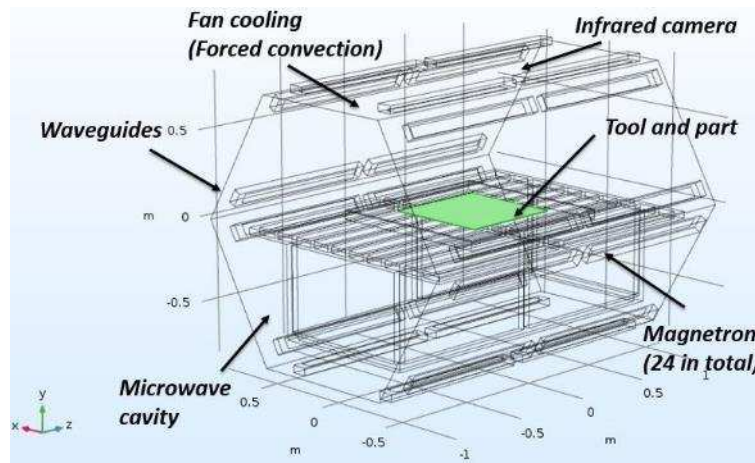


Figure 1 Schematic illustration of the Vötsch microwave cavity with the tool and part in the centre of the cavity

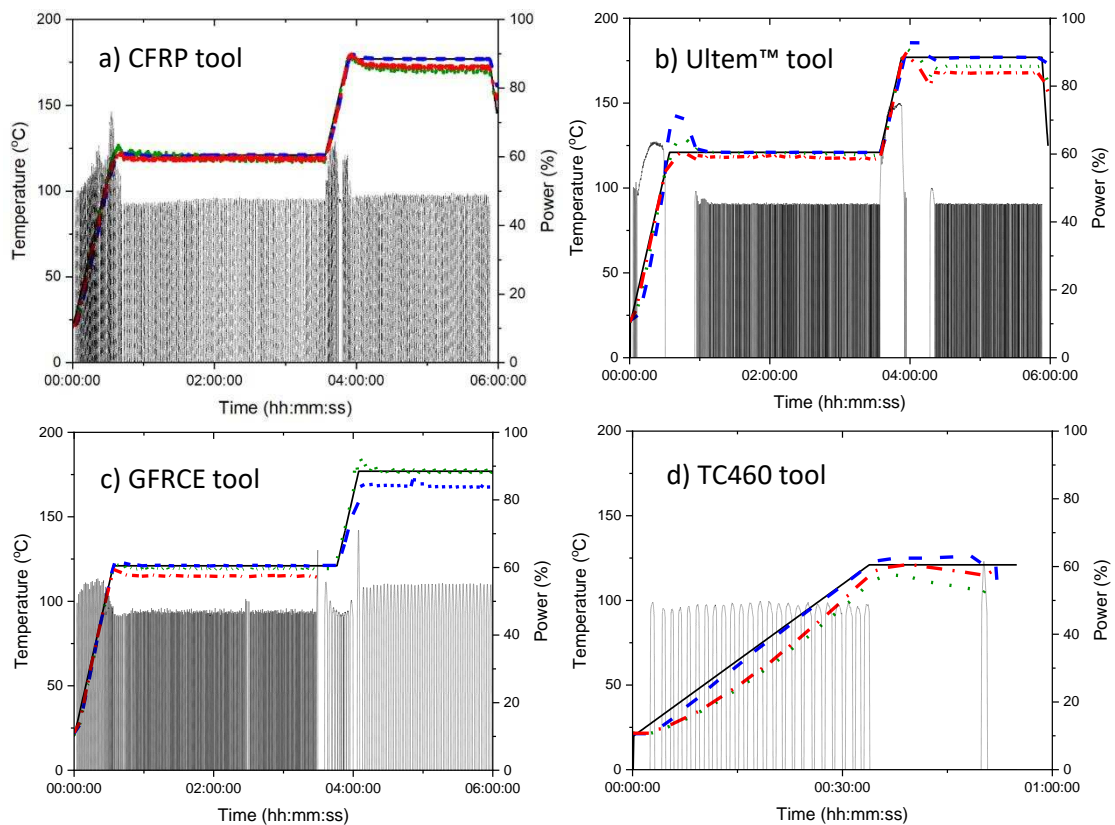


Figure 2 Temperature-time-power graphs of CFRP panels being cured on a) CFRP b) Ultem™ c) GFRCE and d) TC460 tools. The colours/symbols used are temperature (—), power (right axis ---), FOT-A (green), FOT-B (blue) and FOT-C (red)

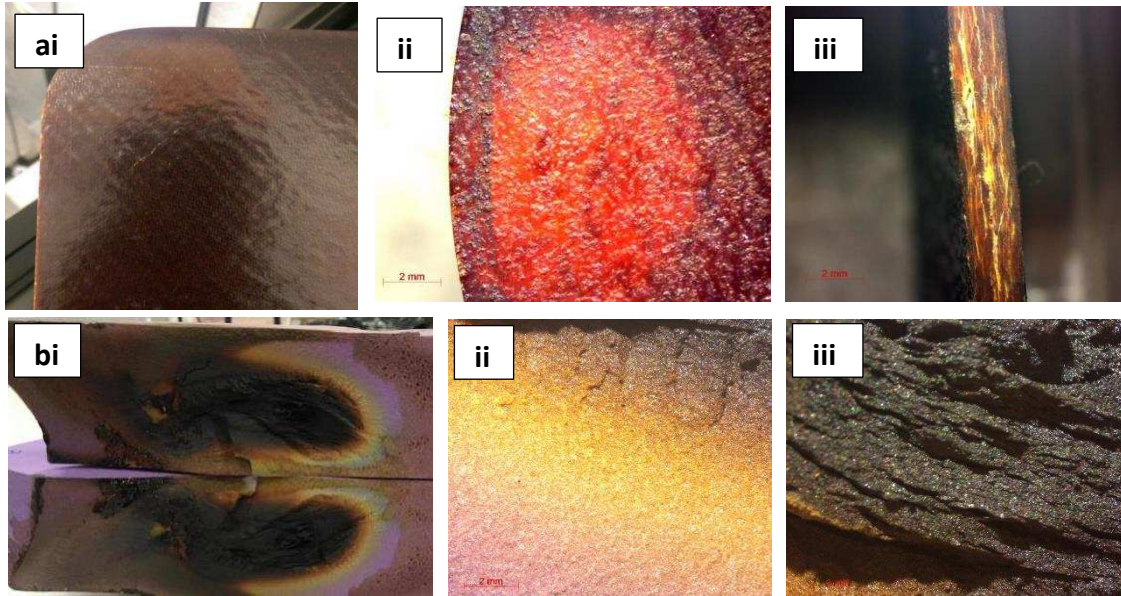


Figure 3 Damage to a) GFRCE and b) TC460 tools at various magnifications (i, ii and iii)

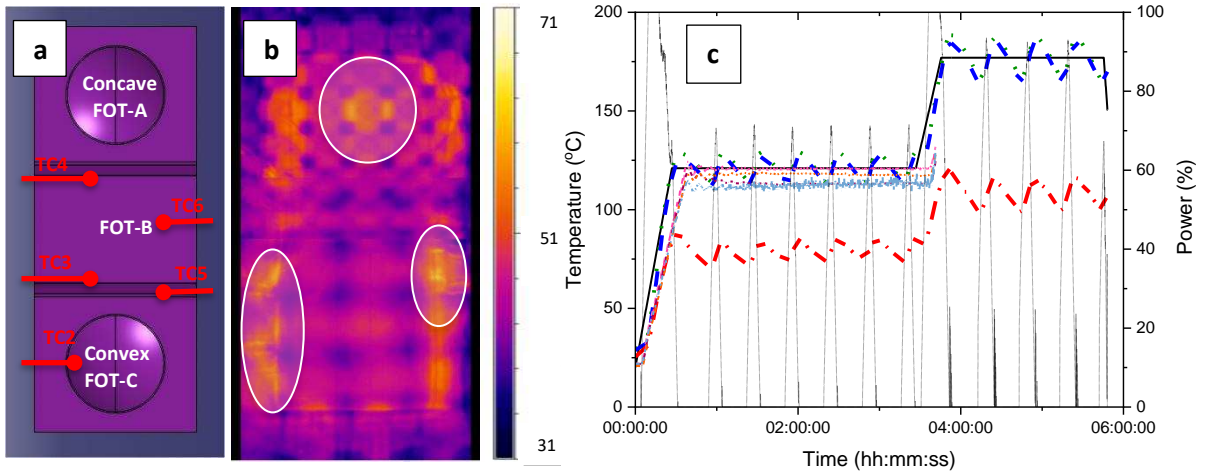


Figure 4 Results for the microwave trials using a CFRP tool, including a) tool geometry outlining the location of thermocouples (TC2-6) and FOT's b) IR image and c) cure cycle (temperature (—), power (right axis ---), TC1 (light pink), TC2 (dark pink), TC3 (brown), TC4 (orange), TC5 (light blue), FOT-A (green), FOT-B (blue) and FOT-C (red))

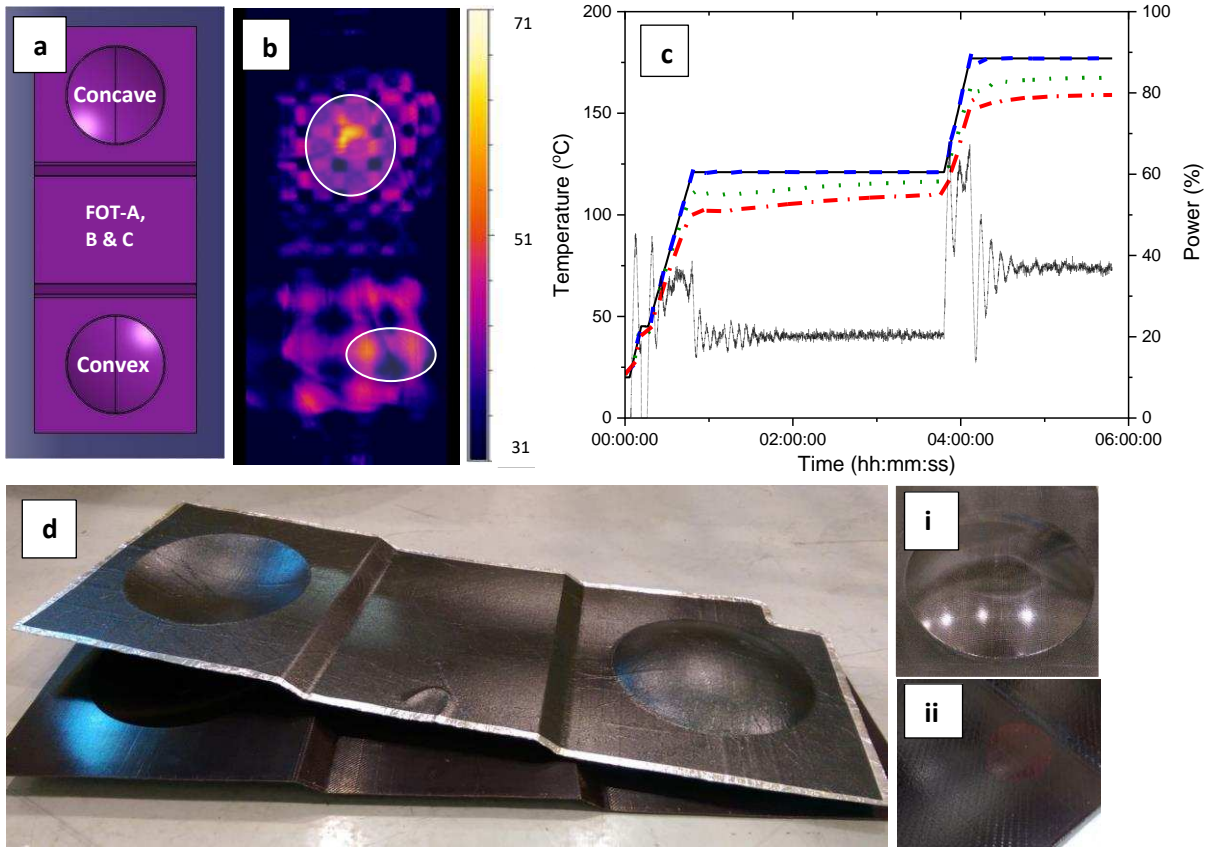


Figure 5 Results for the microwave trials using a GFRCE tool, including a) tool geometry outlining the location of FOT's b) IR image c) cure cycle (temperature (—), power (right axis ---), FOT-A (green), FOT-B (blue) and FOT-C (red)) and d) damage experienced by the panel (i) and tool (ii)

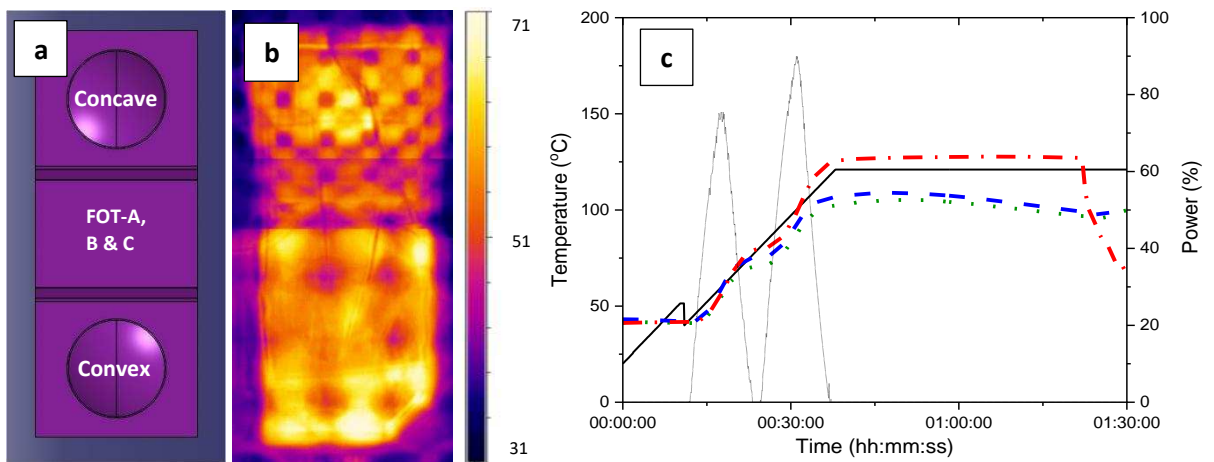


Figure 6 Results for the microwave trials using a TC460 tool, including a) tool geometry outlining the location of FOT's b) IR image c) cure cycle (temperature (-), power (right axis --), FOT-A (green), FOT-B (blue) and FOT-C (red)) and d) damage experienced by the panel (i) and tool (ii)

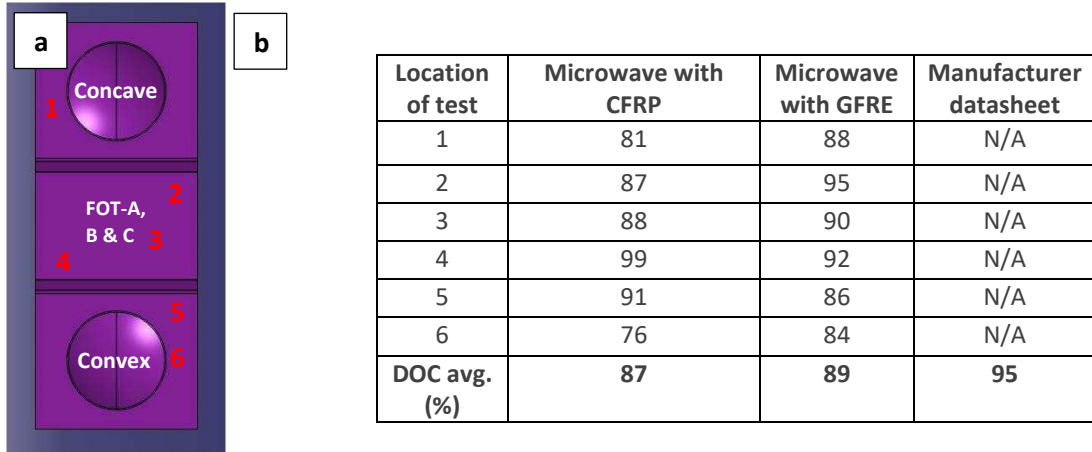


Figure 7 a) Locations of the samples removed from the tools for DOC trials and b) DOC results from each CFRP panel

8. Tables

Table 1 Dielectric and thermal diffusivity properties of selected tooling materials. Highlighted materials were down selected for test bed trials at 2.45 GHz. All tests were conducted at room temperature.

Material	Relative Permittivity ϵ' (-)	Dielectric loss factor ϵ'' (-)	Thermal diffusivity α (mm ² /s)
GFRCE (glass/cyanate ester composite)	4.6	0.040	Axial: 0.282; Rad: 0.422
GFRE (glass fibre/epoxy composite)	4.3	0.054	Axial: 0.257; Rad: 0.281
CFRP/epoxy composite	N/A		Axial: 0.681; Rad: 1.610
TC460 high temp tooling board	1.7	0.006	0.150
Ultem™	3.1	0.011	0.199
Borosilicate glass [32]	4.0	0.001 (calc)	0.536 (calc)
Macor® ceramic [33]	5.9	0.005	0.730 (calc)
PTFE block	1.81	0.000	0.123

Table 2 Summary of how tools performed during the test bed trials (highlighted are the trials taken forward)

Material	Withstand full cycle?	Damage to tool?	Comments
GFRCE (glass/cyanate ester composite)	Yes	Yes	Slight blistering damage to tool
GFRE (glass fibre/epoxy composite)	No	Yes	Voids, moisture absorption and stray fibres
CFRP/epoxy composite	Yes	No	No issues
TC460 high temp tooling board	No	Yes	Location of heating mechanism contributing factor
Ultem™	Yes	No	Difficult to control runaway